A terahertz view on magnetization dynamics

Awari, Nilesh

CHAPTER 2

Introduction to Magnetism

This chapter introduces the basic concepts in magnetism and outlines the current state of the art in light-driven ultra-fast magnetization dynamics. Firstly, an introduction to the origin of magnetic moments in solid materials is provided, followed by a brief description of the properties of magnetic materials. Secondly, the magnetization dynamics of magnetic materials is discussed. The interaction of the magnetization of material with an externally applied field and with femtosecond laser excitation/THz excitation forms the basis of the subject of ultra-fast magnetization dynamics.

2.1 Origin of magnetism and magnetic properties

The spin of a single electron s is the microscopic source of magnetism (in materials). The spin magnetic moment m_s is defined as

$$\boldsymbol{m}_{\mathrm{s}} = \frac{e}{2m} g \boldsymbol{s} \tag{2.1}$$

here e and m are the charge and mass of an electron, g is the gyro-magnetic ratio. s is quantized and has values $\pm$ 1/2. Measurement of the spin magnetic moment yields,

$$m_{s,z} = \pm \frac{1}{2} g \mu_B \tag{2.2}$$

where $\mu_B = \frac{e\hbar}{2m}$ is known as the Bohr magneton, the basic unit of magnetism and magnetic properties of materials are explained using this quantity. For an electron circulating around its nucleus, the total magnetic moment of the electron is given by the combination of its spin s and its orbital angular moment l, (where l is given by the rotational motion of an electron). For material systems with several electrons, the total magnetic moment of the electron system is given by

$$\boldsymbol{J} = \boldsymbol{S} + \boldsymbol{L} \tag{2.3}$$

where $S = \sum_i s_i$ is the total angular spin momentum of the electron system and $L = \sum_i l_{\mathrm{i}}$ is the total angular orbital momentum. The ground state energy of a single atom is defined by Pauli's exclusion principle and Hund's rule [1].

- The state with highest S has the lowest energy, consistent with Pauli's principle
- For a given S, the state with the highest L will have the lowest energy
- For a sub-shell which is not more than half filled, $J = |S - L|$ will have lower energy; for sub-shells more than half filled, $J = |S + L|$ will have lower energy.

The total magnetic moment of such systems is given by,

$$\boldsymbol{m} = -\gamma \boldsymbol{J} \tag{2.4}$$

where γ is the gyro-magnetic ratio. The above discussed Hund's rule explains the magnetic properties of 3d and 4f shell materials where unpaired electrons are localized and shielded by filled electronic states.

For more complex systems where electron wave functions of neighbouring atoms start to overlap, Hund's rule does not give a satisfactory explanation of magnetization. For such cases one needs to consider the contributions from kinetic energy, potential energy, and Pauli's principle to explain parallel or anti-parallel alignment of spin moments. The Hamiltonian of such a system is given by,

$$\mathcal{H} = -\sum_{i \neq j}^{\infty} J_{ij} \boldsymbol{S}_i . \boldsymbol{S}_j \tag{2.5}$$

here J_{ij} is the exchange constant for the Hamiltonian describing the coupling strength of two different spins. The sign of the exchange constant decides parallel (ferromagnetic) or anti parallel (antiferromagnetic) alignment of the spins in the ground state.

Magnetization is defined by, $M = m/V$, with V being the volume of the material under consideration. Magnetic materials are categorized based on the response of the magnetization to the externally applied magnetic field. For materials where no unpaired electrons are present, all spin moments cancel each other resulting in no net magnetization. Such materials show weak magnetization in an external magnetic field which is opposite to the applied magnetic field and are known as diamagnetic materials. On the other hand, materials with unpaired electron spin will react to an external magnetic field and their response can be categorized in five different ways, as indicated in figure 2.1.

Paramagnetic ordering occurs when materials have unpaired electrons resulting in a net magnetic moment. These magnetic moments are randomly aligned as the coupling between different spin moments is weak ($\ll kT$). In the presence of an applied magnetic field, these spin moments are aligned in the same direction as the external magnetic field giving rise to a change in net magnetization. For a system where spin moments are coupled with each other, ferromagnetic ordering (all spins are aligned parallel to each other) or antiferromagnetic ordering (adjacent spins are anti parallel to each other) is observed. The parallel alignment of spins in ferromagnetic materials results in an intrinsic net magnetization even in the absence of an external magnetic field. For ferrimagnetic materials, adjacent spins are of different values. For a canted antiferromagnet, adjacent spins are tilted by a small angle giving rise to a small net magnetization. The canting of spins is explained based on the competition between two processes; namely isotropic exchange and spin-orbit coupling.

Ferromagnetic, antiferromagnetic, and ferrimagnetic materials have a critical temperature above which thermal energy causes randomized ordering of spin moments, resulting in no net magnetization or long range ordering of the spin moments.

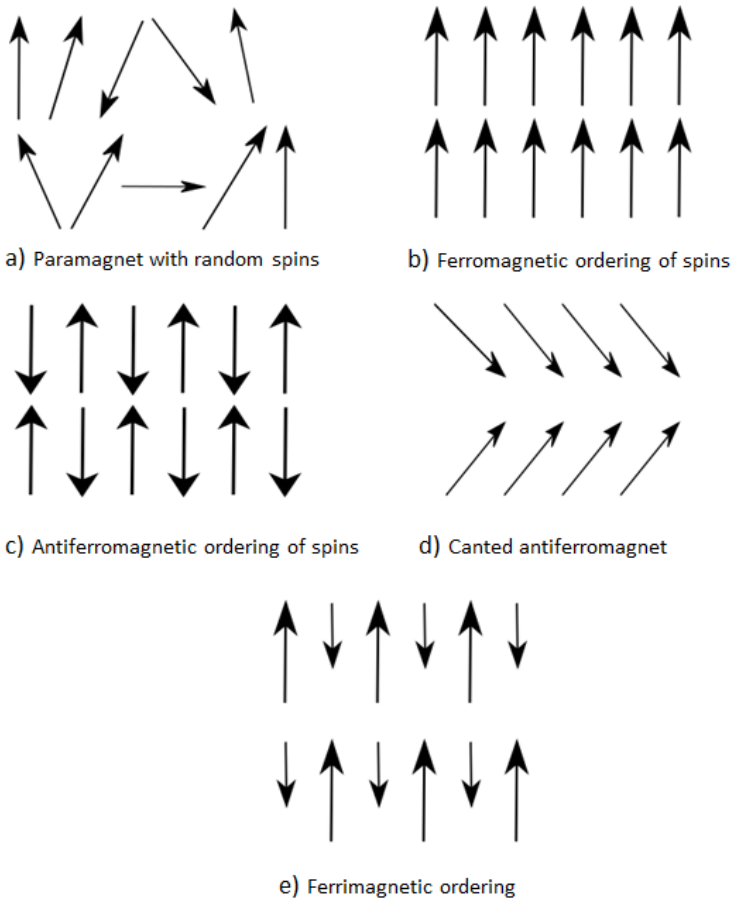

FIGURE 2.1: Different types of magnetic ordering present in materials. Black arrows indicate the direction of magnetic moment, modified from reference [2]

2.2 Magnetic properties of materials

In magnetic materials, magnetic moments have a preferred direction because of the magnetic anisotropy of the materials. The direction along which spontaneous magnetization is directed is known as the easy axis of magnetization. The magnetic anisotropy energy (H_a) can be defined by the following equation,

$$H_a = K_u^2 \sin^2 \theta \tag{2.6}$$

where K_u is the anisotropy constant and θ is the angle between the direction of magnetization ($\boldsymbol{M}$) and the easy axis.

One form of magnetic anisotropy is magneto-crystalline anisotropy, also known as intrinsic anisotropy, which is a result of the crystal field present inside the material. This is the only source of anisotropic energy present for infinite-sized crystals, apart from negligible contributions from the moments generated due to non-cubic symmetry. The

crystal field is the static electrical field present because of surrounding charges. When an electron moves at high speed through such an electric field, in its own frame of reference this electric field is perceived as a magnetic field. This magnetic field interacts with the spin of a moving electron, which is known as spin-orbit coupling. Magneto-crystalline anisotropy can also be generated because of an anisotropic growth of the materials and/or the presence of interfaces.

Another form of magnetic anisotropy occurs because of the shape of the material. The shape anisotropic energy is generally defined as the demagnetizing field as it acts in an antagonistic way to the magnetization which creates it. For a thin rod, the demagnetizing field is smaller if all the magnetic moments lie along the axis of the rod. As the thickness of the rod increases, it is not necessary to have magnetic moments lying along the axis of the rod. For a spherical object, there is no shape magnetic anisotropy as all the directions are equally preferred.

When an external field ($\boldsymbol{B_0}$) is applied to a magnetic material, the magnetization of the material aligns itself parallel to the applied magnetic field. The magnetic potential energy H_{Zeeman} is given by,

$$H_{\text{Zeeman}} = -\boldsymbol{m} \cdot \boldsymbol{B}_0 \tag{2.7}$$

If one considers only the magnetic anisotropy and exchange interactions between the spin moments, then there is degeneracy for the spin direction with lowest energy state. The applied magnetic field can lift this degeneracy and split the electronic states into equally spaced states, which is known as Zeeman splitting. In the Zeeman effect, the external magnetic field is too low to break the coupling between spin magnetic moment and orbital magnetic moment. When higher magnetic fields are applied where this coupling is broken, then splitting is explained using the Paschen-Back effect.

In the presence of an externally applied field, the total magnetic field ($\boldsymbol{B}$) inside the material is given by

$$\boldsymbol{B} = \boldsymbol{B}_0 + \mu_0 \boldsymbol{M} \tag{2.8}$$

where μ_0 is magnetic permeability of free space. The magnetic strength arising from magnetization of the material is $\boldsymbol{H} = \boldsymbol{B_0}/\mu_0$, which when applied to equation 2.8, gives the relation between B, H, and M as;

$$\boldsymbol{B} = \mu_0(\boldsymbol{M} + \boldsymbol{H}) \tag{2.9}$$

For a ferromagnetic material kept in an external magnetic field, the magnetization of the material as a function of applied field is shown in figure 2.2(a). Ferromagnetic materials show saturation magnetization (M_s). This is the maximum magnetization shown by ferromagnetic materials in an applied external field. If one increases the external field further, magnetization of the ferromagnet does not increase. Saturation magnetization is an intrinsic property, independent of particle size but dependent on temperature. Another property of a ferromagnet is that they can retain the memory of an applied magnetic field which is known as the hysteresis effect. The remanent magnetization (M_r) is the magnetization remaining in the ferromagnet when the applied field is restored to zero. In order to reduce the magnetization of a ferromagnet below M_r, a reverse magnetic field needs to be applied, with the magnetization reducing to zero at the coercivity field (H_c).

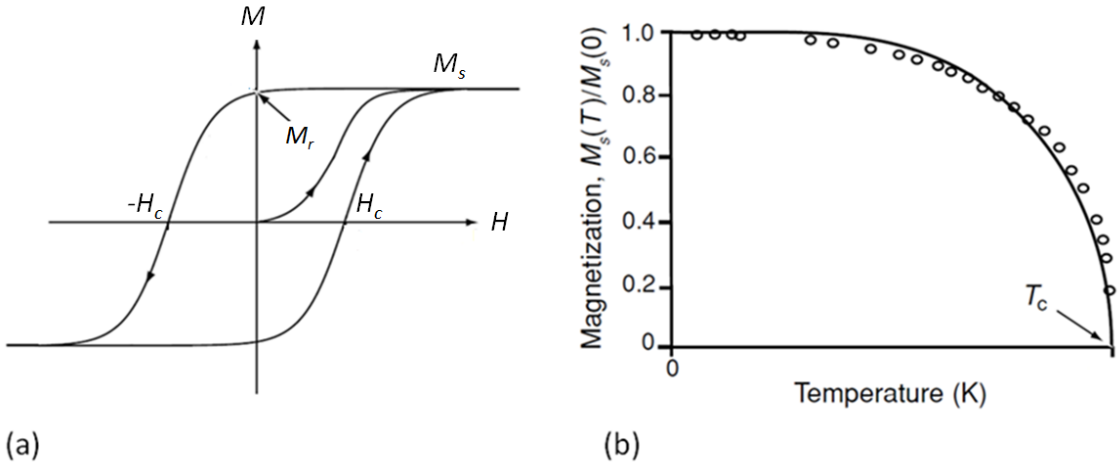

FIGURE 2.2: Properties of a typical ferromagnet, Nickel, taken from [3]. (a) Hysteresis loop observed in Nickel. (b) Temperature dependence of the saturation magnetization for Nickel.

The saturation magnetization of a ferromagnet decreases with increasing temperature and at the critical temperature, known as the Curie temperature (T_C), it goes to 0, see figure 2.2(b). Below T_C, a ferromagnet is magnetically ordered and above T_C it is disordered.

In ferrimagnetic materials, two sub-lattices have different magnetic momenta which gives rise to a net magnetic moment which is equivalent to ferromagnetic materials. Therefore, a ferrimagnetic material shows all the characteristic properties of a ferromagnet such as: spontaneous magnetization, Curie temperatures, hysteresis, and remanence. In an antiferromagnet, the two sub-lattices are equal in magnitude but oriented in opposite directions. The antiferromagnetic order exists at temperatures lower than the Néel temperature (T_N), but at and above T_N the antiferromangetic order is lost.

Magnetic susceptibility is the property of magnetic materials which defines how much a magnetic material can be magnetized in the presence of an applied magnetic field. The magnetic susceptibility of a material is calculated from the ratio of the magnetization M within the material to the applied magnetic field strength H, or $\chi = M/H$. For paramagnetic materials, χ diverges as temperatures approach 0 K (figure 2.3(a)). For ferromagnetic/ferrimagnetic materials χ diverges as the temperature approaches the Curie temperature, as explained by the Curie-Weiss law,

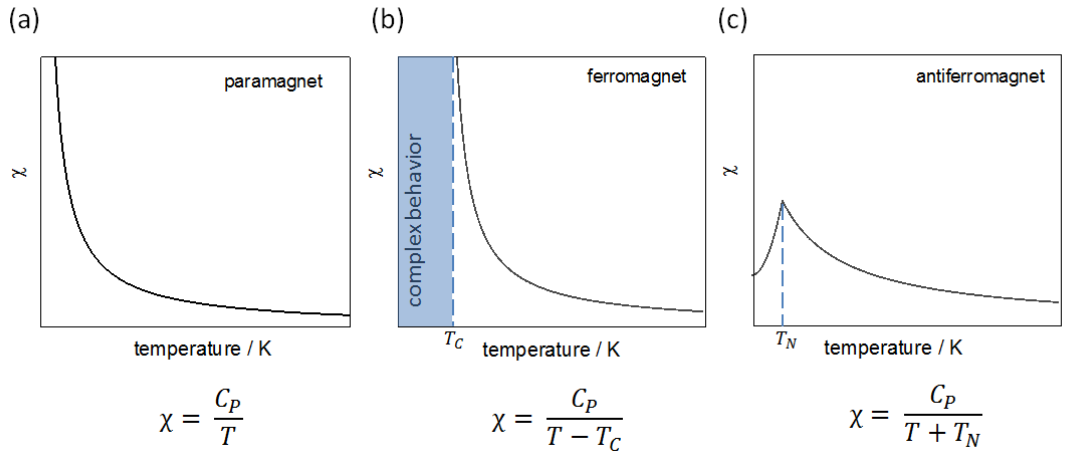

FIGURE 2.3: Susceptibility as a function of temperature for paramagnet, ferromagnet and antiferromagnet is shown, adapted from [4]

.

$$\chi_m = C_P/(T - T_C) \tag{2.10}$$

Here, C_P is the Curie-Weiss constant and T_C is the Curie temperature of the ferromagnetic material. For antiferromagnetic materials (see figure 2.3(c)), χ follows a behavior similar to ferromagnetic materials until the Neel temperature (T_N), below (T_N) it decreases again.

2.3 Ultra-fast magnetization dynamics

The static magnetic properties of a material depend on the time-independent effective magnetization H_{eff} of the material, where H_{eff} is defined as

$$\boldsymbol{H}_{\text{eff}} = \boldsymbol{H}_{\text{ani}} + \boldsymbol{H}_{\text{ext}} + \boldsymbol{H}_{\text{demag}} \tag{2.11}$$

where $\boldsymbol{H}_{\text{ani}}$ is the magnetic anisotropy, $\boldsymbol{H}_{\text{ext}}$ is the externally applied magnetic field, and $\boldsymbol{H}_{\text{demag}}$ is the demagnetizing field present inside the material. When this equilibrium state is perturbed, the magnitude and/or direction of $\boldsymbol{H}_{\text{eff}}$ changes, which causes the magnetization ($\boldsymbol{M}$) of the material to change and relax back to its equilibrium state. Magnetization dynamics can be seen as the collective excitation of the magnetic ground state of the system. For magnetic materials, the elementary excitations, such as electron, spin, and lattice degrees of freedom, become spin-dependent which contributes further to magnetization dynamics [5]. The interaction/coupling of these elementary excitations with magnetic ordering is studied under the scope of magnetization dynamics. With the advancements in femtosecond laser systems, it is now possible to study these interactions on the femtosecond timescale, which has enabled ultra-fast control of magnetization required for spintronics applications. Magnetization dynamics can be categorized into two categories: coherent precessional dynamics and incoherent dynamics.

The coherent precessional dynamics can be explained by the Zeeman interaction of the magnetization of a material with an externally applied field. The magnetic moment undergoes precessional motion when kept in an external magnetic field. Assuming there is no damping involved, the precessional motion of the magnetic moment under consideration is given by the torque ($\boldsymbol{T}$) acting on the magnetic moment,

$$\boldsymbol{T} = \boldsymbol{m} \times \boldsymbol{H}_{eff} \tag{2.12}$$

Torque is the rate of change of the angular momentum ($\boldsymbol{L}$),

$$\boldsymbol{T} = \frac{d}{dt}\boldsymbol{L} \tag{2.13}$$

The magnetic moment of an electron is directly proportional to its angular momentum through γ (gyro-magnetic ratio with the value of 28.02 GHz/T for a free electron).

$$\boldsymbol{m} = -\gamma \boldsymbol{L} \tag{2.14}$$

The time derivative of the above equation yields,

$$\frac{d\boldsymbol{m}}{dt} = -\gamma \frac{d\boldsymbol{L}}{dt} = -\gamma \boldsymbol{T} \tag{2.15}$$

Including the classical expression of torque in the above equation and considering the magnetic anisotropy, and the demagnetizing field present in the system, the above equation can be modified to

$$\frac{d\boldsymbol{m}}{dt} = -\gamma \boldsymbol{m} \times \boldsymbol{H}_{eff} \tag{2.16}$$

Equation 2.16 is the Landau-Lifschitz (LL) equation for magnetization dynamics. This equation only considers the precessional motion of the magnetization. In order to account for motion of the magnetization toward alignment with the field, a dissipative term is introduced by Gilbert. A new equation including a dissipative term is known as the Landau-Lifschitz-Gilbert (LLG) equation and is as below;

$$\frac{d\boldsymbol{m}}{dt} = -\gamma \boldsymbol{m} \times \boldsymbol{H}_{eff} + \frac{\alpha}{M_s} \boldsymbol{m} \times \frac{d\boldsymbol{m}}{dt} \tag{2.17}$$

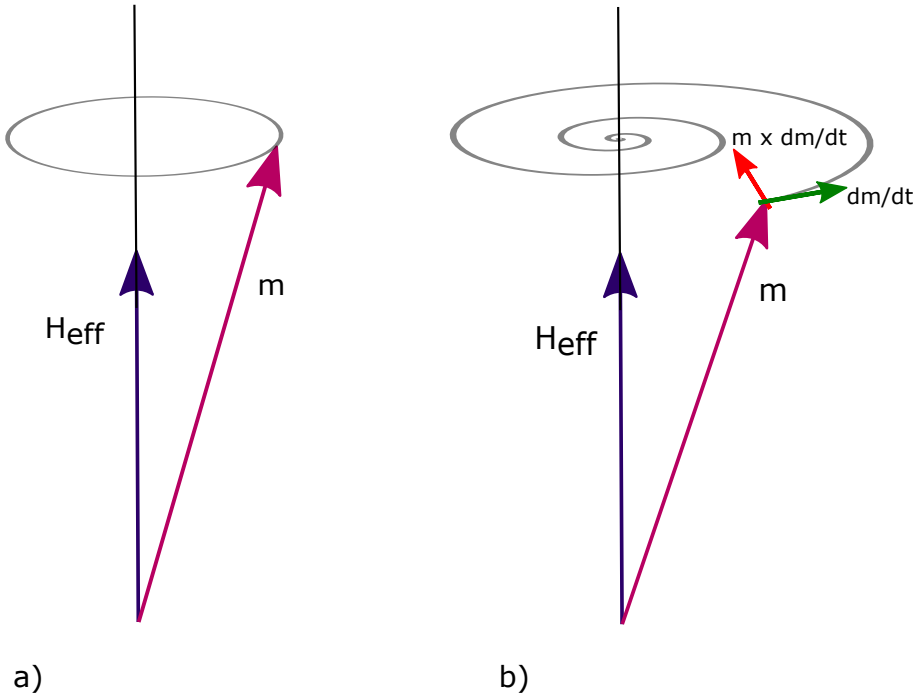

FIGURE 2.4: Schematic of the magnetic precession (a) without damping and (b) with damping.

where α is the dimensionless Gilbert damping constant. The LLG equation can also be used in the atomistic limit to calculate the evolution of the spin system using Langevin dynamics to model ultra-fast magnetization processes [6]. The frequency of the precession is normally in the GHz range and the time required to reach the equilibrium state can be as high as nanoseconds, depending on the damping mechanism.

Another way to disturb the static magnetic properties of a material is by irradiating it with femtosecond near infra-red (NIR) optical pulses. In this case, the electron absorbs part of the laser energy and achieves a non-equilibrium state. The thermal energy provided by the ultra-fast laser perturbs the spin ordering resulting in demagnetization

of the magnetic system. The demagnetization takes place during the first few 100 fs after laser excitation. This timescale is orders of magnitude shorter than the timescale involved in coherent precessional dynamics. The first observation of ultra-fast demagnetization of Ni [7] by ultra-short laser pulses has shown a demagnetization time of less than 1 ps. Laser induced magnetization dynamics can be divided into coherent interactions [8] and incoherent demagnetization. In order to explain the incoherent demagnetization process, the Elliot-Yafet (EY) type spin flip mechanism has been used. The EY scattering based on electron-phonon scattering [9, 10] has been most widely used. In the EY mechanism, electron spins relax via momentum scattering events because of spin-orbit coupling (SOC). In the presence of SOC, electronic states are admixtures of spin up and spin down states because of which, at every scattering event of electrons, there is a small but finite probability of spin-flip.

In order to interpret ultra-fast demagnetization, the 3-temperature model (3TM) [7, 9] based on electron-phonon scattering was developed. In this model, the interactions between 3 thermal baths which are in internal thermal equilibrium is explained. The electron bath temperature T_{el}, spin bath temperature T_{sp}, and lattice temperature T_{lat} are coupled to each other via thermal coupling constants as shown in the equations below [7]:

$$C_{el}\frac{dT_{el}}{dt} = -G_{el,lat}(T_{el} - T_{lat}) - G_{el,sp}(T_{el} - T_{sp}) + P(t) \tag{2.18}$$

$$C_{lat}\frac{dT_{lat}}{dt} = -G_{lat,sp}(T_{lat} - T_{sp}) - G_{el,lat}(T_{el} - T_{lat}) \tag{2.19}$$

$$C_{sp}\frac{dT_{sp}}{dt} = -G_{el,sp}(T_{sp} - T_{el}) - G_{lat,sp}(T_{sp} - T_{lat}) \tag{2.20}$$

Here, *P(t)* is the excitation laser pulse, C is the heat capacities of the three systems and G is the coupling constant between the three systems. The thermalization process of these three thermal baths upon laser excitation is summarized as follows (also see figure 2.5):

1. The laser beam hits the sample and creates electron-hole pairs on a time scale of $\sim$ 1 fs, which results in heating of the electron system (ultra-fast process)

2. Electron-electron interaction reduces the electronic temperature (T_{el}) within the first few 100 fs, depending on the material under investigation

3. Electron-phonon interaction relaxes the electronic excitation in 0.1 to 10 ps which increases the temperature of the lattice (T_{lat})

4. The electron-spin interactions or lattice-spin interactions are responsible for the demagnetization of the magnetic materials.

In order to gain a deeper understanding of ultra-fast demagnetization, one needs to understand how angular momentum conservation takes place.

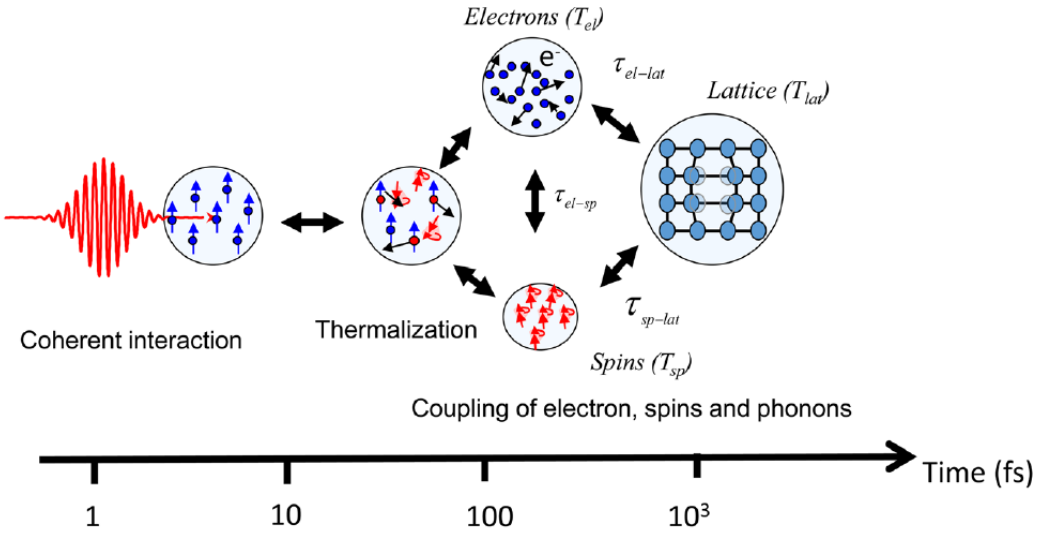

FIGURE 2.5: Schematic of time scales involved in laser driven excitation of magnetic materials over 1 ps time scale. The thermalization processes between electrons and spins are shown after 50-100 fs. Thermalization process for the lattice is taking place on the timescale 1 ps and higher. Taken from [11].

Figure 2.5 shows the various processes occurring after irradiation of ferromagnetic materials with femtosecond NIR pulses. The coherent excitation of charge and spin occurs in the first few femtosecond after irradiation with NIR pulses, which leads to a non-thermalized distribution. The thermalized distribution is reached on a 50 femtosecond timescale, whereas the thermalization process involving phonons takes place on the time scale of 1 picosecond and higher. Upon laser excitation, non equilibrium hot carriers are generated. These hot carriers result in spin-dependent transport and their distribution in the magnetic materials is spatially inhomogeneous, which affects the optical response of the material. The excited hot carrier dynamics can be categorized into local and non-local physical processes.

One of the important local effects of excited hot carriers is spin-flip scattering, which is considered to be an important factor in explaining ultra-fast laser-induced demagnetization observed in magnetic systems. Spin-flip scattering is the process in which the angular momentum of the local spin is transferred to the lattice or to impurity sites

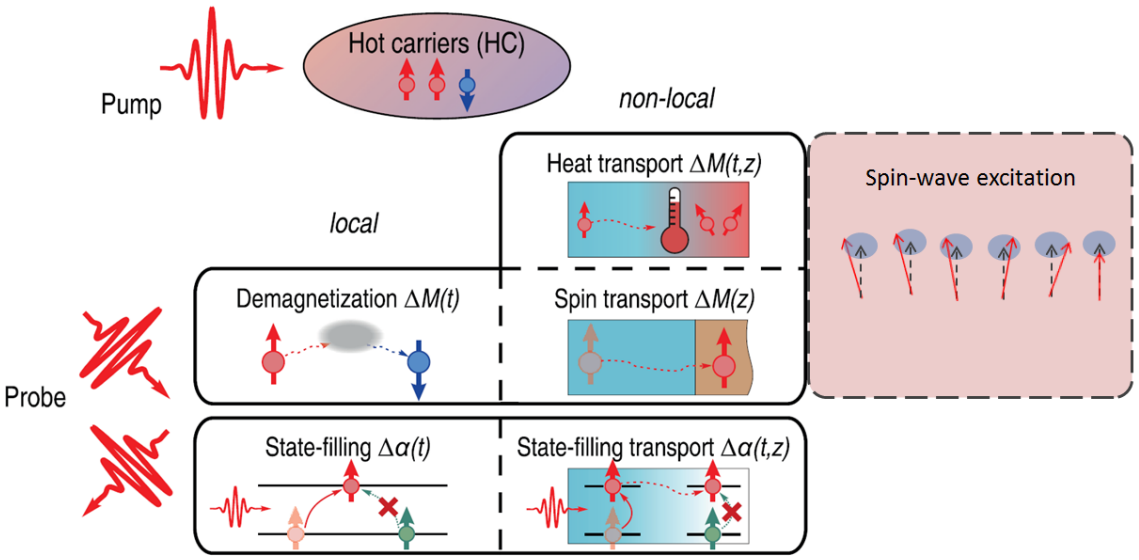

FIGURE 2.6: Effect of femtosecond laser excitation in the near infrared regime on magnetic materials. The excited hot carriers undergo local and non local physical processes which determine the magnetization dynamics of the material. The local effects includes; hot carriers populating empty electronic states and the spin flip scattering. In the non-local effects, inhomogeneous distribution of hot carriers enable spin-polarized super-diffusive spin transport. The magneto-optical response of the material is a combination of both local and no-local effects taking place upon laser excitation. Figure adapted from [12].

[7, 9, 10], thus changing the effective magnetization of the system locally. The timescale of demagnetization is predicted under the assumption that the speed of demagnetization is defined by the speed of spin-flip under the Elliot-Yafet mechanism [11, 13]. Apart from the demagnetization, excited hot carriers also contribute to state-filling effects because of the strong non-equilibrium distribution of hot carriers. The state filling effects are also spin-dependent in nature and results in a transient magneto-optical signal. This could also excite spin waves/magnon modes in a magnetic materials with the frequency of magnetic modes present in the material.

The excited hot carriers exhibit spin-dependent transport across the magnetic material because of the inhomogeneous distribution of hot carriers. This transport can be modelled with a two-channel model [14, 15] with separate channels for transport of spin up and spin down electrons. This enables spin-polarized super-diffusive current in magnetic materials [16–18]. A thermally driven spin-polarized current originates from different Seebeck coefficients in the two spin channels. The super-diffusive transport changes the spin distribution in a magnetic material which changes the magnetization of the material. The super-diffusive transport is considered as spin conserving, which means that there is no spin flip taking place during the transport of a spin from one place to an other. There have been multiple experiments showing the existence of both the processes but their relative contribution is still under debate. Despite the intense research

in the field of ultra-fast demagnetization, the mechanism responsible for dissipation of angular momentum on sub-picosecond timescale is not clear. In order to explain the experimental results, a variety of theoretical models have been proposed that aimed to model the large complexity of NIR femtosecond laser-induced highly non-equilibrium state. Recently, intense THz radiation has been used to induced demagnetization in ferromagnetic materials [19–22]. With THz excitation, the electronic temperature is slightly increased whereas with NIR excitation the electronic temperature is higher than 1000 K [23]. Because of a lower electronic temperature, individual electron scattering becomes dominant over electronic cooling [22]. In this experimental approach, THz pulses drive spin current in ferromagnetic systems [19, 24] and it has been shown that the inelastic spin scattering is of the order of $\sim$ 30 fs [19].

This thesis discusses the experimental studies where low energy THz radiation is used to excite, control, and manipulate the magnetization of materials on ultra-fast timescales.

2.4 Bibliography

[1] D. J. Griffiths, *Introduction to quantum mechanics*. Cambridge University Press, 2016.

[2] J. S. Miller, "Organic-and molecule-based magnets," *Materials Today*, vol. 17, no. 5, pp. 224–235, 2014.

[3] J. M. Coey, *Magnetism and magnetic materials*. Cambridge University Press, 2010.

[4] Z.-F. Guo, K. Pan, and X.-J. Wang, "Electrochromic & magnetic properties of electrode materials for lithium ion batteries," *Chinese Physics B*, vol. 25, no. 1, p. 017801, 2015.

[5] A. Eschenlohr, U. Bovensiepen, *et al.*, "Special issue on ultrafast magnetism," *Journal of Physics: Condensed Matter*, vol. 30, no. 3, p. 030301, 2017.

[6] R. F. Evans, W. J. Fan, P. Chureemart, T. A. Ostler, M. O. Ellis, and R. W. Chantrell, "Atomistic spin model simulations of magnetic nanomaterials," *Journal of Physics: Condensed Matter*, vol. 26, no. 10, p. 103202, 2014.

[7] E. Beaurepaire, J.-C. Merle, A. Daunois, and J.-Y. Bigot, "Ultrafast spin dynamics in ferromagnetic nickel," *Physical review letters*, vol. 76, no. 22, p. 4250, 1996.

[8] J.-Y. Bigot, M. Vomir, and E. Beaurepaire, "Coherent ultrafast magnetism induced by femtosecond laser pulses," *Nature Physics*, vol. 5, no. 7, p. 515, 2009.

[9] B. Koopmans, G. Malinowski, F. Dalla Longa, D. Steiauf, M. Fähnle, T. Roth, M. Cinchetti, and M. Aeschlimann, "Explaining the paradoxical diversity of ultrafast laser-induced demagnetization," *Nature materials*, vol. 9, no. 3, p. 259, 2010.

[10] B. Koopmans, J. Ruigrok, F. Dalla Longa, and W. De Jonge, "Unifying ultrafast magnetization dynamics," *Physical review letters*, vol. 95, no. 26, p. 267207, 2005.

[11] J. Walowski and M. Münzenberg, "Perspective: Ultrafast magnetism and thz spintronics," *Journal of applied Physics*, vol. 120, no. 14, p. 140901, 2016.

[12] I. Razdolski, A. Alekhin, U. Martens, D. Bürstel, D. Diesing, M. Münzenberg, U. Bovensiepen, and A. Melnikov, "Analysis of the time-resolved magneto-optical kerr effect for ultrafast magnetization dynamics in ferromagnetic thin films," *Journal of Physics: Condensed Matter*, vol. 29, no. 17, p. 174002, 2017.

[13] S. Günther, C. Spezzani, R. Ciprian, C. Grazioli, B. Ressel, M. Coreno, L. Poletto, P. Miotti, M. Sacchi, G. Panaccione, *et al.*, "Testing spin-flip scattering as a possible mechanism of ultrafast demagnetization in ordered magnetic alloys," *Physical Review B*, vol. 90, no. 18, p. 180407, 2014.

[14] A. Slachter, F. L. Bakker, and B. J. van Wees, "Modeling of thermal spin transport and spin-orbit effects in ferromagnetic/nonmagnetic mesoscopic devices," *Physical Review B*, vol. 84, no. 17, p. 174408, 2011.

[15] T. Valet and A. Fert, "Theory of the perpendicular magnetoresistance in magnetic multilayers," *Physical Review B*, vol. 48, no. 10, p. 7099, 1993.

[16] M. Battiato, K. Carva, and P. M. Oppeneer, "Superdiffusive spin transport as a mechanism of ultrafast demagnetization," *Physical review letters*, vol. 105, no. 2, p. 027203, 2010.

[17] K. Carva, M. Battiato, D. Legut, and P. M. Oppeneer, "Ab initio theory of electron-phonon mediated ultrafast spin relaxation of laser-excited hot electrons in transition-metal ferromagnets," *Physical Review B*, vol. 87, no. 18, p. 184425, 2013.

[18] E. Turgut, J. M. Shaw, P. Grychtol, H. T. Nembach, D. Rudolf, R. Adam, M. Aeschlimann, C. M. Schneider, T. J. Silva, M. M. Murnane, *et al.*, "Controlling the competition between optically induced ultrafast spin-flip scattering and spin transport in magnetic multilayers," *Physical review letters*, vol. 110, no. 19, p. 197201, 2013.

[19] S. Bonetti, M. Hoffmann, M.-J. Sher, Z. Chen, S.-H. Yang, M. Samant, S. Parkin, and H. Dürr, "Thz-driven ultrafast spin-lattice scattering in amorphous metallic ferromagnets," *Physical review letters*, vol. 117, no. 8, p. 087205, 2016.

[20] M. Shalaby, C. Vicario, and C. P. Hauri, "Low frequency terahertz-induced demagnetization in ferromagnetic nickel," *Applied Physics Letters*, vol. 108, no. 18, p. 182903, 2016.

[21] M. Shalaby, C. Vicario, and C. P. Hauri, "Simultaneous electronic and the magnetic excitation of a ferromagnet by intense THz pulses," *New Journal of Physics*, vol. 18, no. 1, p. 013019, 2016.

[22] D. Polley, M. Pancaldi, M. Hudl, P. Vavassori, S. Urazhdin, and S. Bonetti, "Thz-driven demagnetization with perpendicular magnetic anisotropy: Towards ultrafast ballistic switching," *Journal of Physics D: Applied Physics*, vol. 51, no. 8, p. 084001.

[23] H.-S. Rhie, H. Dürr, and W. Eberhardt, "Femtosecond electron and spin dynamics in Ni/W (110) films," *Physical review letters*, vol. 90, no. 24, p. 247201, 2003.

[24] Z. Jin, A. Tkach, F. Casper, V. Spetter, H. Grimm, A. Thomas, T. Kampfrath, M. Bonn, M. Kläui, and D. Turchinovich, "Accessing the fundamentals of magnetotransport in metals with terahertz probes," *Nature Physics*, vol. 11, no. 9, p. 761, 2015.